

## AERODYNAMIC ANALYSIS OF THE CLARK YH AIRFOIL

Vasile PRISACARIU

“Henri Coandă” Air Force Academy, Brasov, Romania (prisacariu.vasile@afahc.ro)  
ORCID: 0000-0003-4370-4756

DOI: 10.19062/1842-9238.2021.19.1.4

**Abstract:** *The analysis of the performance of aerodynamic airfoils leads to optimized approaches regarding the pre-design of fixed and rotating lifting surfaces, with implications on the global characteristics and performances of aircraft. The 2D aerodynamics of the airfoils provides indications on the aeromechanical behavior of the selected geometric elements, which may come as constructive solutions depending on the typology of the missions and the initial requirements of the project.*

*The article provides a scrutiny of and certain educational perspectives on the Clark YH profile analysis, using freeware tools (Javafoil, Profili and XFLR5).*

**Keywords:** *Clark YH, aerodynamic analysis, Javafoil, Profili, XFLR5.*

### Acronims and symbols

AoA	Angle of attack	CNC	Computer numerical control
XFLR	Xfoil low Reynolds	LLT	Lifting line theory
$C_m$	Pitch coefficient	$C_d$	Drag coefficient
$C_p$	Pressure coefficient	$C_l$	Lift coefficient
$C_l / C_d$	Gliding ratio		

## 1. INTRODUCTION

### 1.1 The geometry of the aerodynamic airfoil

The aerodynamic airfoil is characterized by the following geometric elements (figure 1.1): airfoil chord ( $c$ ), maximum arrow of the profile skeleton ( $f_{\max}$ ), position of the maximum arrow, defined by the distance from the leading edge ( $a_f$ ), maximum airfoil thickness ( $e_{\max}$ ), the position of the maximum thickness, defined by the distance from the leading edge ( $a_e$ ), the radius of curvature of the leading edge ( $r$ ), the angle at the leading edge,  $\tau$ . [1, 2].

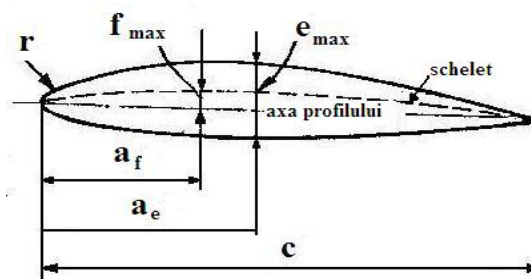
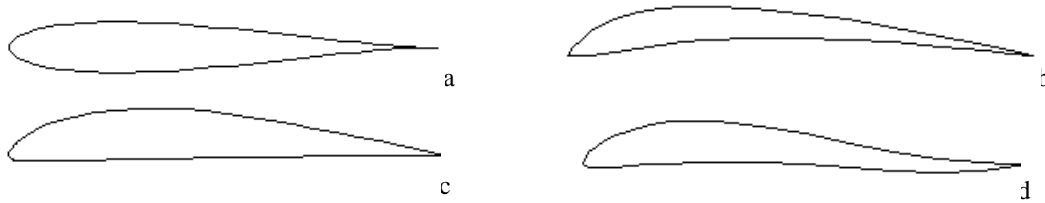


FIG.1.1 Airfoil geometric elements

*Airfoil classification*

It can be after *the curvature* (figure 1.2): symmetrical airfoils, asymmetrical airfoils (plane-convex, biconvex, concave-convex, double-curvature); according to *the shape* of the skeleton and the flight board: Zhukovsky, Carafoli, von Misses, Karmann-Trefftz; by *speed range* (subsonic, supersonic).



**FIG. 1.2** Airfoil types (a.biconvex-simetric, b.concave-convex, c.plane-convex, double curvature)

The airfoils can also be classified according to *the elaboration method*, they can be: *theoretical airfoils*, obtained by conforming transformations, or by inversion of some curves (basic theoretical airfoils, Jukovski airfoils, Jukovski-Betz airfoils, Karman-Trefftz airfoils, Betz-Keune airfoils, Carafoli airfoils); *empirical airfoils*, obtained by free tracing or choosing accordingly equations for skeleton shape and thickness distribution (EC airfoils, EQ airfoils, ECH airfoils, EQH airfoils, NACA-NASA airfoils, Gottingen airfoils, TAGHI airfoils, ONERA airfoils, Clark Y airfoils, RAF airfoils, RAE airfoils, *profiles obtained with inverse methods*, starting from the imposed pressure distributions (supercritical airfoils, superlifting airfoils, airfoils for low speeds).

**1.2 Criteria for choosing airfoils**

Choosing the class of wing and tail airfoils, correctly establishing the airfoils that will generate the aerodynamic surfaces of the aircraft are complex problems, the correct solution of which depends directly on the level of performance and flight qualities of the designed aircraft. [3]

The value of the  $C_{lmax}$  coefficient of the wing without flaps is of interest in establishing the maneuverability of aircraft with acrobatic characteristics. It is important to consider the lifting component at incidences close to that corresponding to the maximum lifting capacity.

Another important parameter is the value of the  $C_{dmin}$  coefficient. The maximum flight speed, the maximum flight distance, the fuel consumption over a given distance, etc. depend on this value.

The zero lifting moment coefficient,  $C_{m0}$ , intervenes in the degree of stress of the wing structure and in the equilibrium conditions around the pitch axis, affecting the horizontal tail lift at equilibrium and in the corresponding turning tail range. For these reasons it is preferable to have a airfoils whose coefficient  $C_{m0}$  is zero or as small as possible.

The requirements presented are contradictory and cannot be equally satisfied by the same type of airfoils, because of this they will be preferentially satisfied depending on the category of the aircraft.

**2. OBJECT OF THE ANALYSIS AND SOFTWARE INFORMATION**

**2.1 The Clark YH airfoil**

The airfoil for aerodynamic analysis (figure 1.3) is derived from Clark Y, has the characteristics shown in Table 1.1 and is often used in the construction of flying wings due to stability characteristics (due to reflex flight board) but also low speed aircraft in classic aerodynamic configuration.

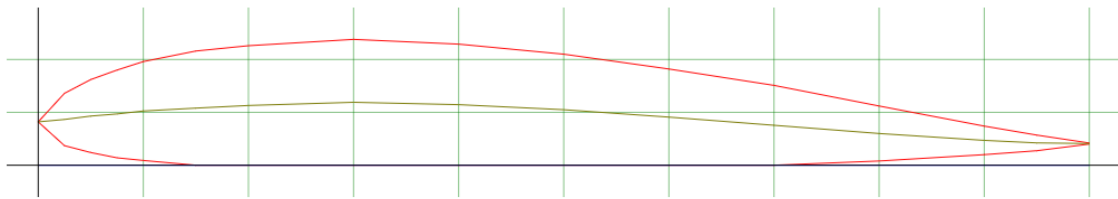


FIG. 1.3 Clark YH airfoil, [4, 16].

Table 1.1 Clark YH airfoil characteristics

Characteristics	Values	Characteristics	Values
Max. thickness	11,9 % la 30% x/c	Max. AoA	9°
AoA at $C_{d0}$	-2.0	AoA at $(C_l/C_d)_{max}$	4.5°
Max. arrow	5.95% at 30% x/c	$C_{l,max}$	1.11
$(C_l/C_d)_{max}$	32.834	$C_l$ at $(C_l/C_d)_{max}$	0.683

The types of aircraft using the Clark YH profile are shown in Figure 1.4.



FIG. 1.4 Aircrafts using the Clark YH airfoil, a. Curtiss F9C-2 Sparrow-Hawk (1932) [5], b. YAK 12 (1947) [6], c. Hawker Hurricane (1937) [7], d. Miles M14 Magister (1939), [8].

## 2.2 SOFTWARE USED FOR THE AERODYNAMIC ANALYSIS

### 2.2.1 Javafoil

JavaFoil is a relatively simple software, which uses several traditional methods for aerodynamic analysis, the most important being the analysis of the potential flow and the analysis of the boundary layer (figure 2.1). The analysis of the potential flow is based on the panel method (linear distribution of variable vorticity). Taking a set of profile coordinates, it calculates the local flow rate (no viscosity) along the airfoil surface for any angle of attack, [9, 10].

The analysis of the boundary layer is applied on the upper and lower surfaces of the airfoil, starting from the stagnation point. It solves a set of differential equations to find the different parameters of the boundary layer (integral method).

The equations and criteria for transition and separation are based on the procedures described by Eppler [11, 12, 16].

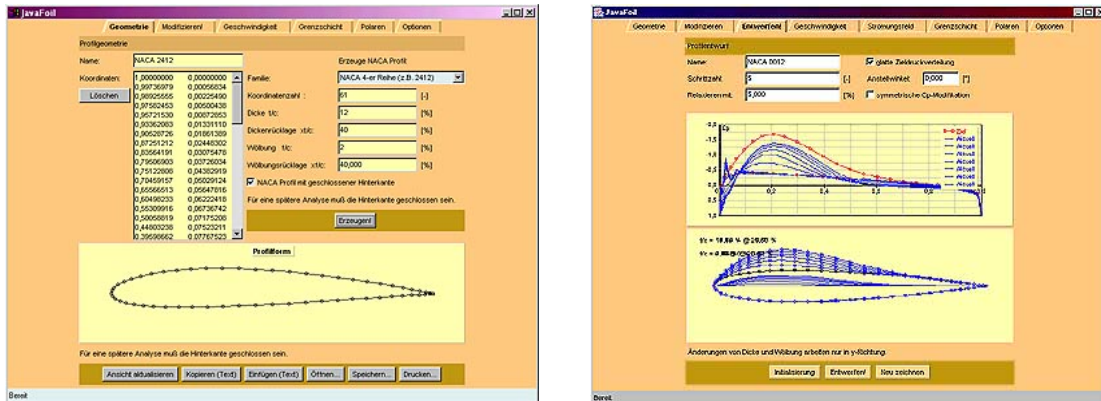


FIG. 2.1 Graphical user interface - Javafoil

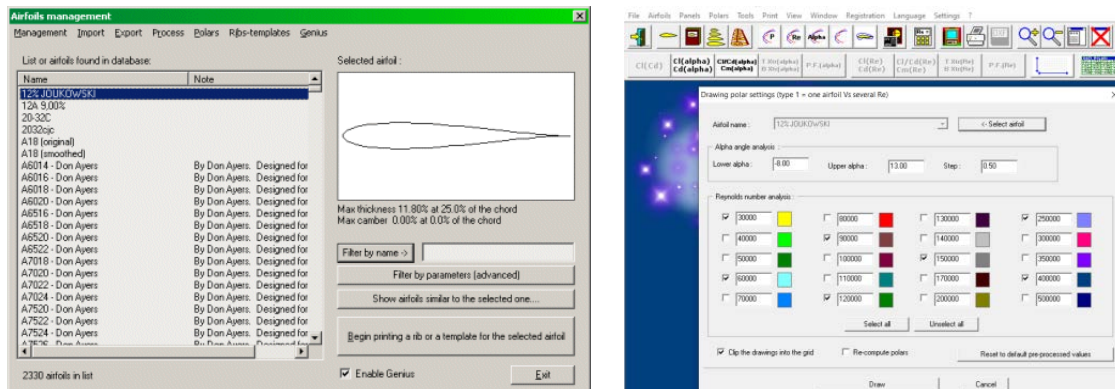
Javafoil also contains specific tools for geometric parameterization depending on the thickness, arrow and curvature of the airfoils. 2D geometries can be generated or imported from external databases.

Both step analyzes (potential flow and boundary layer analysis) are applied for an angle of attack (AoA) interval, which gives a complete polar of the airfoil for a Reynolds number. The calculations are performed by your own computer code (not by Eppler or XFOIL). Only the boundary layer module was based directly on the method found in the initial version of the Eppler program.

JavaFoil is a relatively simple software with limitations. Because JavaFoil does not model laminar flow separation bubbles and turbulent flow separation, the results will be incorrect if large flow separation areas are present. Mass separation, as in the stall mode, is modeled to some extent by empirical corrections, so that the maximum lift can be predicted approximately for "conventional" airfoils. If you analyze an air airfoil beyond this regime, the results will be quite inaccurate.

2.2.2 Profili

Profili software has a database of over 2,200 aerodynamic profiles with precomputed aerodynamic characteristics, which minimizes the time in performing aerodynamic comparisons (figure 2.2). The user can modify the geometry of the airfoil both by modifying the global characteristics (thickness, curvature) and the local characteristics by applying a flap of curvature, [13].



a. airfoil database

b.parameter (AoA și Re) for polars

FIG. 2.2 GUI Profili – airfoil aerodynamic analysis

The software tool has a series of functions of geometric parameterization and aerodynamic analysis grouped on a series of modules, as follows: airfoil geometry management (import/export of airfoils from / to external databases); airfoil geometry processing; polar generation regarding aerodynamic coefficients ( $C_l$ ,  $C_d$ ,  $C_m$ ,  $C_p$ ); geometric definitions (ribs, wings) for plotting and CNC making and routing (foam panels), see figure 2.3. Profili software contains facilities for exporting geometries in various formats (\* .dxf, \* plt, \* pro, \* .dat, \* .cor) and polarities (\* .html).

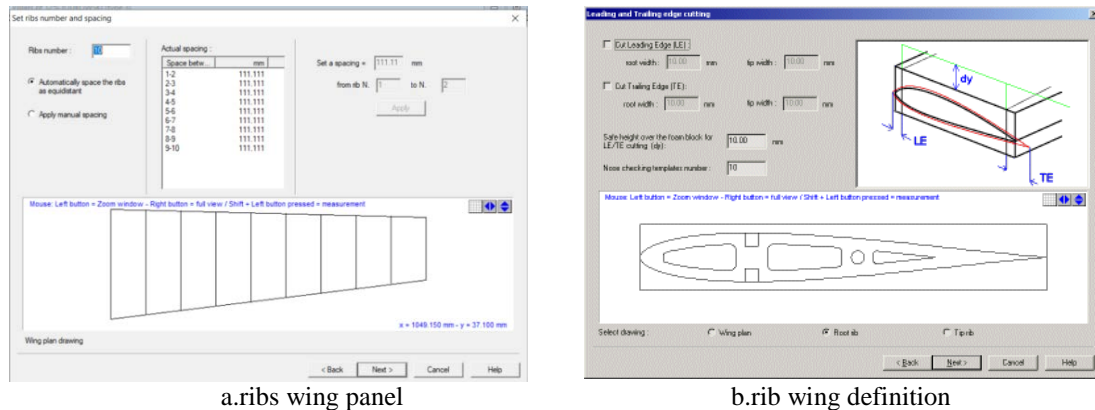


FIG. 2.3 GUI Profili software– wing geometry

### 2.2.3 XFRL5

XFRL5 is compatible with Windows operating systems using Microsoft MFC libraries, and use in Linux, MAC and Unix requires an emulator.

It is an aerodynamic analysis software tool based on a code valid only for non-propelled models (gliders), for which it provides reasonable results. Therefore, the approach to geometries similar to real aircraft is limited, regardless of the influence of propellers, [14]. XFRL5 is based on five basic modules: two modules for geometric parameterization of initiation and comparison of airfoil (B-Splines); the mode with reverse design routines (mixed-QDES and total-MDES) of the airfoil; direct airfoil analysis module (OPER); how to analyze the wings, fuselage and glider, (Fig. 2.4).

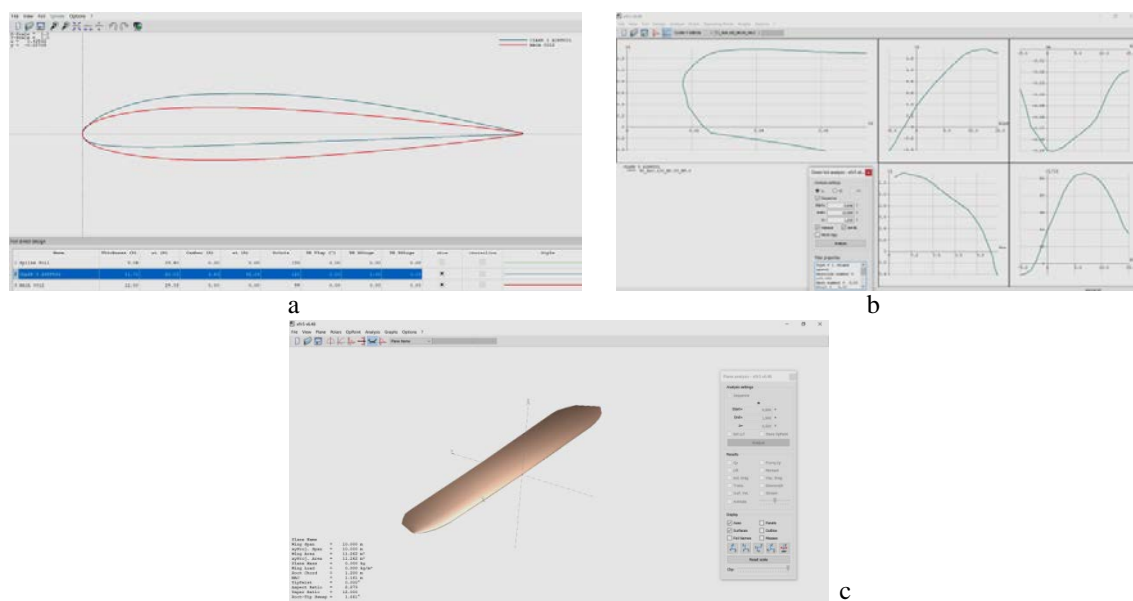


FIG. 2.4 XFRL5 modules, a. geometrical module - airfoil, b.direct analysis module - airfoil, c. geometrical module -wing

The numerical analysis methods underlying the software code are: lifting line theory (LLT); vortex lattice method (VLM) and panel method. [15]

### 3. AERODYNAMIC ANALYSIS

#### 3.1 Conditions for the analysis

The aerodynamic analyses are based on the theoretical characteristics of the Clark YH airfoil in table 1.1, and the analysis conditions used by the three software tools (Javafoil, Profiles, XFLR5) are recorded in table 3.1.

*Table 3.1. Conditions of analysis*

Conditions	Value	Conditions	Value
Angle of attack (AoA)	$-5^{\circ} \div 13^{\circ}$	Speed	10 ÷ 30 m/s
Nr. Reynolds	$2 \times 10^5 / 4 \times 10^5 / 6 \times 10^5$	Density	1,22 kg/m <sup>3</sup>
Iterations	100	Viscosity	$1,5 \times 10^{-5}$ m <sup>2</sup> /s

#### 3.2 Numerical results and interpretations

We present the graphical aspects of the numerical results depending on the software tool, according to the analysis matrix in table 3.2.

*Table 3.2. Cases of analysis*

Polars / graphs	Javafoil	Profili	XFLR5
$C_l$ vs $C_d$	▬ ▬ ▬	▬ ▬ ▬	▬ ▬ ▬
$C_l$ vs AoA	▬ ▬ ▬	▬ ▬ ▬	▬ ▬ ▬
$C_d$ vs AoA	-	▬ ▬ ▬	▬ ▬ ▬
$C_m$ vs AoA	▬ ▬ ▬	▬ ▬ ▬	▬ ▬ ▬
$C_l/C_d$ vs AoA	-	▬ ▬ ▬	▬ ▬ ▬

#### 3.2.1 Javafoil

The results of the analyses with Javafoil software are highlighted in figures 3.1 ÷ 3.3.

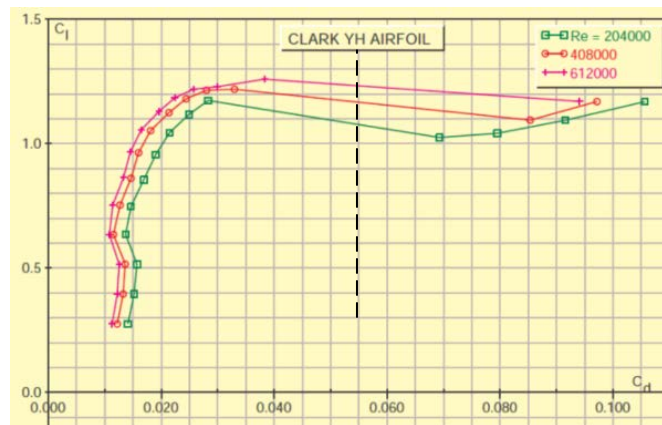


**FIG. 3.1** Polarels  $C_l$ - $C_d$  - Javafoil

Figure 3.1. shows comparative variations of  $C_l$  vs  $C_d$  coefficient for the three Reynolds numbers, the lift coefficient ( $C_l$ ) decreases with the decrease of the Reynolds number at a fixed  $C_d$  value, and with the increase no. Reynolds AoA maximum increases, (fig. 3.2) while the value  $C_m$  is quasi-constant and reveals a self-stable behavior of the airfoil (fig.3.3).

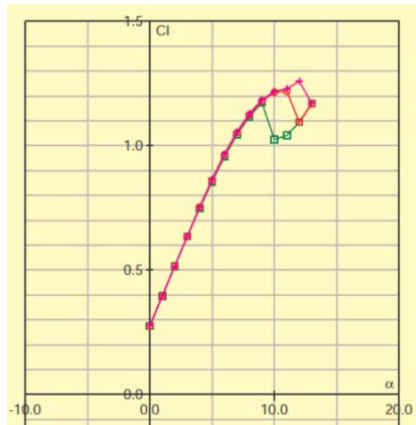


FIG. 3.2 Polar  $C_l$ -AoA - Javafoil

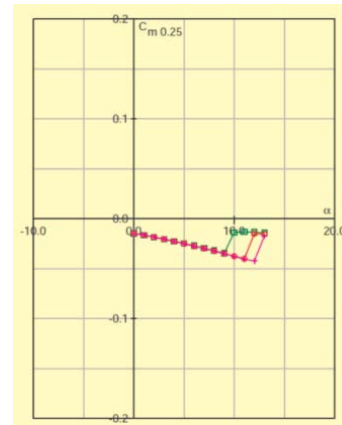


FIG. 3.3 Polar  $C_m$ -AoA - Javafoil

### 3.2.2.Profili

Figures 3.4 ÷ 3.6 provide the most relevant characteristic polars of the analyzed airfoil (without flap junction).



FIG. 3.4 Polar  $C_l$ - $C_d$  - Profili

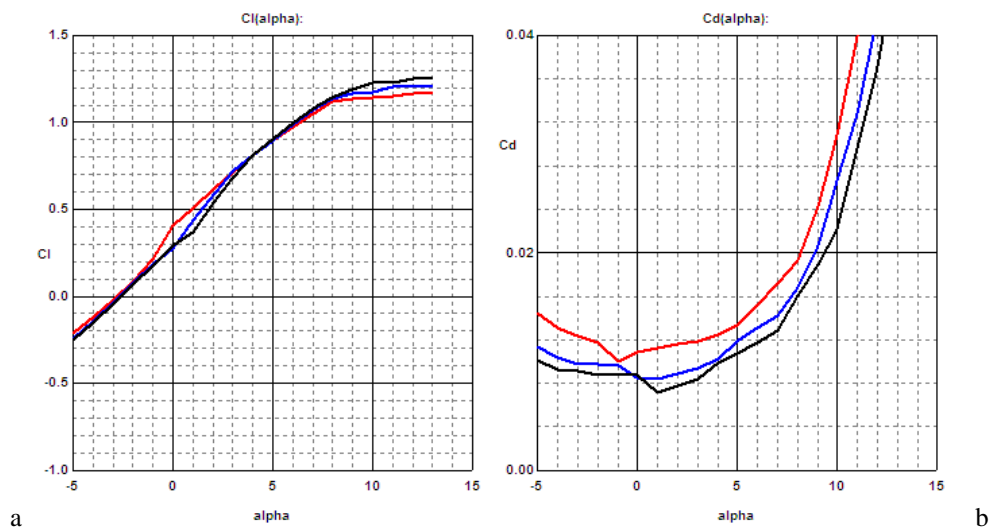
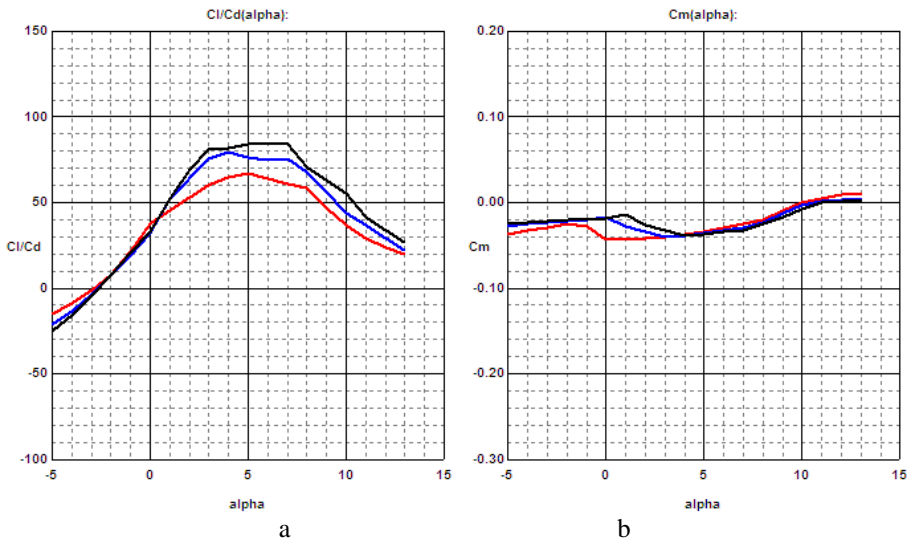


FIG. 3.5 Polars a. $C_l$ -AoA, b. $C_d$ -AoA - Profili

Figure 3.5a shows identical polar corresponding to the three flight speeds, the lift coefficient has a maximum value (1.25) at an incidence of  $13^\circ$ , and the drag coefficient has a significant linear increase starting with an incidence of  $7^\circ$ .



**FIG. 3.6** Polar  $C_l/C_d$ -AoA (a),  $C_m$ -AoA - Profili

Figure 3.6a shows a maximum gliding ratio ( $C_l/C_d$  -AoA) at the incidence of  $7^\circ$  to  $30$  m/s,  $4^\circ$  to  $20$  m/s and  $5^\circ$  to  $10$  m/s, while the pitch coefficient ( $C_m$ ) it has almost zero value ( $-0,0001$ ) at the incidence of  $10^\circ$ , and after  $11^\circ$  positive values are observed ( $0.005$ ). Maximum negative values ( $-0.0414$ ) of the pitch coefficient are recorded at the incidence of  $2^\circ$  for the speed of  $10$  m/s.

### 3.2.3 XFLR5 analysis

Figures 3.7 ÷ 3.9 provide the characteristic polars, the most relevant of the analyzed airfoil (without flap).

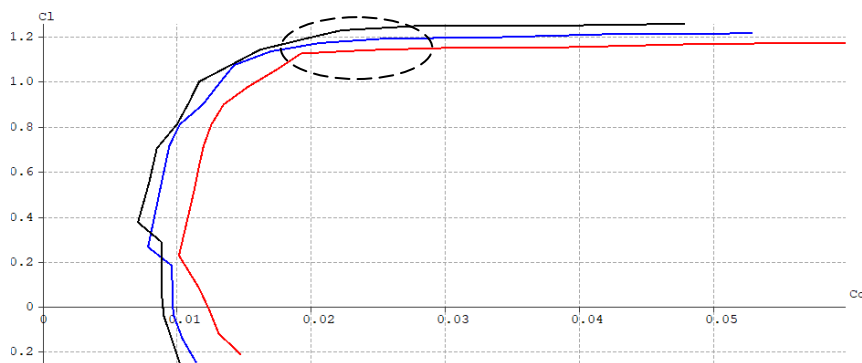


**FIG. 3.7** Polar  $C_l$ - $C_d$  – XFLR5

Variations of the  $C_d$  value are observed for  $C_l=1.15 \div 1.2$  (figure 3.7) and for  $AoA > 5^\circ$  (figure 3.8b), while the lifting behavior is similar over the whole incidence range (AoA), figure 3.8a.

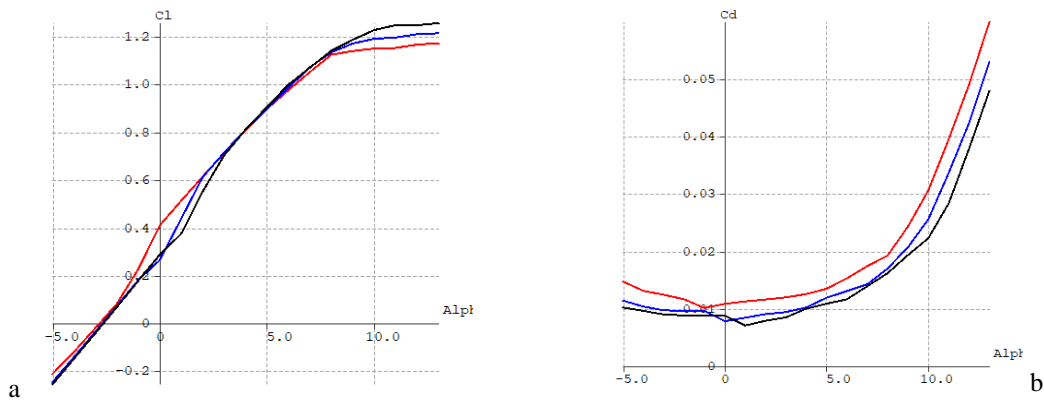


FIG. 3.8 Polars a.  $C_l$ -AoA, b.  $C_d$ -AoA – XFLR5

According to figure 3.9a the maximum gliding ratio corresponds to  $AoA = 5^\circ$ , and  $C_m$  reveals a self-stable behavior for the three Reynolds numbers (according to the sign convention).

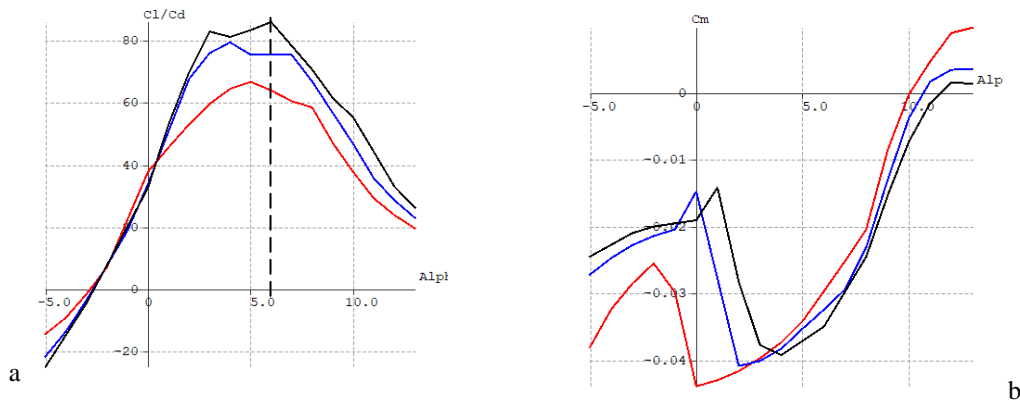


FIG. 3.9 Polars  $C_l/C_d$ -AoA (a),  $C_m$ -AoA - Profili

For a complete image and a verification of the numerical analyzes we proceeded to a comparative stage of the values generated by the three software tools, for no.  $Re = 204,000$ , according to figure 3.10.

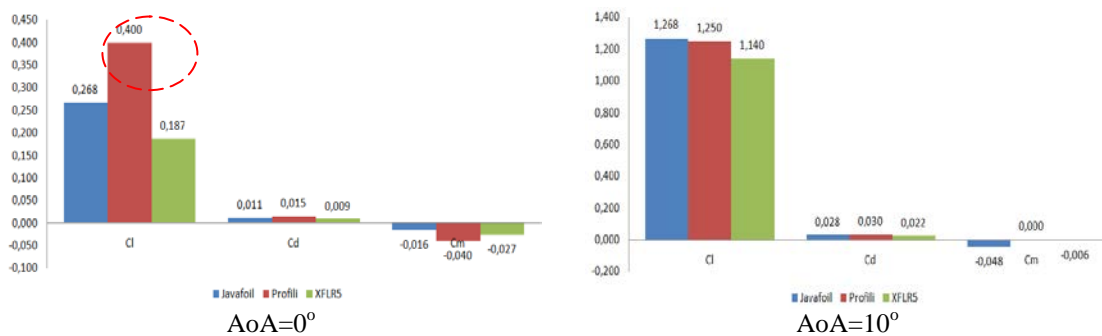


FIG. 3.9 Comparative values of coefficients  $C_l$ ,  $C_d$  și  $C_m$

We observe differences of the numerical values for the coefficient  $C_l$  due to the calculation errors of the Profili software for the zero angle of attack (see also figure 3.8a). For the other values we observe irrelevant differences of the calculated coefficients.

## CONCLUSIONS

Aerodynamic analysis tools based on open source numerical codes can be used in the online or offline environment with a series of geometric options (number of points, setting flap) that provide the user with a complete analysis matrix similar to real cases.

The three selected aerodynamic analysis software provide educational and pre-design approaches to 2D geometries generating relevant qualitative results but limited quantitative results. The use of freeware based on different numerical codes provides a complete picture of the aerodynamic behavior for aerodynamic profiles.

Last but not least, the approach of aerodynamic analysis with the help of a series of software tools offers the opportunity to evaluate the source codes underlying the concept of numerical simulations, giving users the opportunity to seek improvements.

## ACKNOWLEDGMENTS

This article was produced with the support of the documentation of the complex project, acronym MultiMonD2, code PNIII-P1-1.2-PCDDI-2017-0637, contract 33PCDDI/2018 funded by UEFISCDI.

## REFERENCES

- [1] C. Rotaru, *Aerodinamică - Elemente teoretice și aplicații*, Editura Academiei Tehnice Militare, ISBN 978-973-640-186-2, 272 pag., 2009;
- [2] F.W. Riegels, *Aerofoil sections – Results from wind-tunnel investigations theoretical foundations*, London 1961, U.D.C. Number: 533.6.01, 292p, <https://www3.nd.edu/~ame40462/RiegelsAerofoilSections.pdf>;
- [3] D. Newman, *Interactive aerospace engineering and design*, 2002, ISBN 0-07-234820-8, McGraw-Hill Series in Aeronautical and Aerospace Engineering, New York, SUA, 374p;
- [4] Airfoiltools, online database, <http://airfoiltools.com/airfoil/details?airfoil=clarkyh-il>, accessed on 12.04.2021;
- [5] [https://airandspace.si.edu/collection-objects/curtiss-f9c-2-sparrowhawk/nasm\\_A19410007000](https://airandspace.si.edu/collection-objects/curtiss-f9c-2-sparrowhawk/nasm_A19410007000), accessed on 02.05.2021;
- [6] [https://en.wikipedia.org/wiki/Yakovlev\\_Yak-12#/media/File:Jak-12\\_PICT0025.JPG](https://en.wikipedia.org/wiki/Yakovlev_Yak-12#/media/File:Jak-12_PICT0025.JPG), accessed on 02.05.2021;
- [7] [https://ro.wikipedia.org/wiki/Hawker\\_Hurricane#/media/Fi%C8%99ier:Hurricane.r4118.arp.jpg](https://ro.wikipedia.org/wiki/Hawker_Hurricane#/media/Fi%C8%99ier:Hurricane.r4118.arp.jpg), accessed on 12.05.2021;
- [8] [https://en.wikipedia.org/wiki/Miles\\_Magister#/media/File:Aircraft\\_of\\_the\\_Royal\\_Air\\_Force\\_1939-1945-\\_Miles\\_M.14\\_Magister.\\_CH140.jpg](https://en.wikipedia.org/wiki/Miles_Magister#/media/File:Aircraft_of_the_Royal_Air_Force_1939-1945-_Miles_M.14_Magister._CH140.jpg), accessed on 12.05.2021;
- [9] Javafoil software, <https://www.mh-aerotoools.de/airfoils/javafoil.htm>, accessed on 12.05.2021;
- [10] M. Heperle, *Javafoil user's guide*, 45.p, 2017, disponibil la <https://www.mh-aerotoools.de/airfoils/java/JavaFoil%20Users%20Guide.pdf>;
- [11] T. Mueller, et al.: *Low Reynolds Number Wind Tunnel Measurements: The Importance of being Earnest*, Conference on Aerodynamics at Low Reynolds Numbers, London, 1986;
- [12] R. Eppler, and D. Somers, *A Computer Program for the Design and Analysis of Low-Speed Airfoils*, NASA TM-80210, 1980;
- [13] S. Duranti. *Profili 2.21 software*, 2012, Feltre-Italia, [www.profil2.com](http://www.profil2.com), accessed on 12.05.2021;
- [14] M. Drela, Yungren H., *Guidelines for XFLR5 v6.03 (Analysis of foils and wings operating at low Reynolds numbers)*, 2011, available at <http://sourceforge.net/projects/xflr5/files>;
- [15] Katz & Plotkin, “*Low Speed Aerodynamics, From wing theory to panel methods*”, Cambridge University Press, 2nd Ed. 2001;
- [16] V. Prisacariu, *The aerodynamic analysis of the profiles for flying wings*, JOURNAL OF DEFENSE RESOURCES MANAGEMENT, vol.4 issue 1(6)/2013, ISSN:2068-9403, eISSN:2247-6466, ISSN-L: 2247-6466, p211-218.